Available online at www.sciencedirect.com
SCIENCE DIRECT®
ELSEVIER
Journal of the European Ceramic Society 26 (2006) 2249–2255
ECERS
www.elsevier.com/locate/jeurceramsoc

Effect of ageing on microstructure changes in EB-PVD manufactured standard PYSZ top coat of thermal barrier coatings

A. Flores Renteria, B. Saruhan *

German Aerospace Centre, Institute of Materials Research, Cologne D-51147, Germany

Received 10 December 2004; received in revised form 29 March 2005; accepted 14 April 2005
Available online 21 June 2005

Abstract

The ceramic top coat of thermal barrier coatings (TBC) manufactured by electron beam-physical vapour deposition (EB-PVD) process is a crucial part of a system which protects the high pressure turbine blades of aero engines and stationary gas turbines. Under service conditions, turbine blades are exposed to temperatures above 1100 °C, typically with short-term peaks. Ceramic top coat has a unique microstructure made up of individual primary columns, growing in a preferred crystal direction. This columnar growth produces an inter-columnar spacing exhibiting a weak bonding between the neighbouring columns, and providing the TBCs with high strain tolerance. Rotation of the substrates during vapour phase deposition produces an additional intra-columnar closed porosity. Furthermore, this causes formation of a feather-like sub-columnar structure at the periphery of each primary column due to over-shadowing, increasing total porosity and thus contributing to low thermal conductivity of the material.

On thermal exposure during service, both inter- and intra-columnar porosity decrease as a result of sintering induced surface area reduction. The driving force for this process is the decrease in surface energy. As a result, thermal conductivity increases due to the alteration of the porosity distribution, size and morphology. In addition the in-plane strain tolerance decreases after the primary columns sinter together to form bridges at the contact points. These are two important factors which affect the performance of the entire system. Thus, analysis of the involvement of each pore family (feather-arm, intra- and inter-columnar pores) in thermal insulating capabilities of yttria stabilized zirconia (PYSZ) TBC may provide a guideline for engine manufacturers in designing more efficient coatings with optimised thermal properties, in all probability solely by controlled adjustment of the process parameters.

This work reports the thermal-induced microstructural changes in terms of total porosity at EB-PVD produced top coats before and after annealing at 900 °C, 1000 °C, 1100 °C, 1200 °C, 1300 °C and 1400 °C for 1 h, as well as at 1100 °C for 20 min, 1 h, 3 h, 10 h and 100 h. For the analysis of the changes in pore surface area, methods such as SANS (small angle neutron scattering) and BET (Brunauer–Emmett–Teller) were applied. Alteration of surface area with time and temperature commonly gives an indication of the type of diffusion mechanism. Hence, kinetic and the activation energy of the mechanism are calculated and determined with the help of the data obtained by SANS and BET-analysis. Due to the presence of a large number of nano-sized closed porosity in the coatings, SANS measurements were crucial to distinguish those from the remaining open porosity. A mean porosity representative for pores smaller than 180 nm is obtained by interaction of neutrons diffracting parallel to the primary column axis.

Keywords: Sintering; Diffusion; Porosity; ZrO_2; EB-PVD-coatings; Thermal barrier coatings

Abbreviations: SANS, small angle neutron scattering; SAND, small angle neutron diffraction; IPNS, Intense Pulsed Neutron Source of Argonne National Laboratory, USA; BET, Brunauer–Emmett–Teller surface area analysis; EB-PVD, electron beam-physical vapour deposition process; PYSZ, partially yttria stabilized zirconia; TBC, thermal barrier coatings; TGO, thermal grown oxide layer; BC, bond coat; FE-SEM, field-emission scanning electron microscope; ASAP 2010, accelerated surface area porosimeter system

* Corresponding author.
E-mail address: bilge.saruhan@dlr.de (B. Saruhan).

0955-2219/$ – see front matter © 2005 Elsevier Ltd. All rights reserved.
doi:10.1016/j.jeurceramsoc.2005.04.027

1. Introduction

Thermal barrier coating (TBC) systems manufactured by electron beam-physical vapour deposition (EB-PVD) process are currently employed to protect the turbine blades located at the high pressure zone of aero engines and stationary gas turbines. A TBC-system consists of a ceramic top coat, a metallic bond coat (BC) and in between them a thermally grown oxide layer (TGO). The ceramic top coat exhibits a low thermal conductivity and high values of strain tolerance owing to its intrinsic columnar microstructure. This morphology contains individual columns which grow on the substrate in a preferred crystallographic direction by adding atoms from the vapour phase. The columns are weakly connected with each other forming inter-columnar open porosity due to the presence of the gap between them. Furthermore, a feather-like sub-columnar structure which forms at the periphery of the primary column surfaces 45°–60° inclined toward their growing axis increases the open porosity. Finally, due to the rotation of the specimens during the vapour deposition process, the secondary columns, so-called feather-arms which lay inwards to the columns, as well as an additional intra-columnar closed porosity inside the primary columns are produced. Sintering of these coatings, caused by ageing during service conditions, introduces changes in the distribution and morphology of the open and closed porosity, consequently resulting in an increase of the thermal conductivity which is one of the key functional properties of TBCs. Additionally, the in-plane strain tolerance is reduced after the columns sinter together through bridging contact points.[1,2]

According to the sintering theory of Kingery,[3] there are several parallel reaction paths likely to occur, the one with the lowest energy barrier being the most rapid and the principal contributor to the overall process. Following this principle, if there is one single diffusion mechanism governing the surface area changes of the porosity present at the EB-PVD top coats, it may be possible to determine this by measuring the surface area reduction after ageing. It can be assumed that the changes caused by ageing in the morphology of the gaps between feather-arms are comparable to the sintering of particles having analogous morphologies. Moreover, for intra-columnar pores, such changes could be similar to particles or pores with non-equilibrium morphology.

Analysis of the surface area changes could be done by utilizing German's kinetic equation derived from the Kuczynski's format which is time-dependant for surface area reduction. This sintering model assumes that powder particles are monodispersed spheres and the limit of applicability is up to $\Delta S/S_o \approx 50\%$.[4] Alternatively, it is also possible to apply a kinetic model based on Arrhenius analysis developed by German[5,6] which considers the changes in the surface area related to the ageing temperature during constant heating rate. Also this model is only valid for the first 50% of area loss and assumes that a single diffusion mechanism is operative during sintering. In the German's model the slope of the Arrhenius plot represents the values of Q/γ, where γ is the coefficient corresponding to the relevant sintering mechanism produced by the atomic diffusion and Q is the related activation energy.

Small angle neutron scattering technique (SANS) has been employed to study the sintering of ceramics.[7–14] Particularly, the studies focus on measurements of Porod scattering[15] which are derived from the terminal slope in SANS spectra and are used to determine the characteristics of voids in a porous material yielding quantitative information on the corresponding interface surface area. Porod scattering is a technique which does not require a void shape model and is especially useful for studies of void systems with complex shapes.[16] This analysis method is sensitive to both opened and closed pores.[17] Nevertheless, the measured Porod surface area is primarily sensitive to small pores (which have larger surface-to-volume ratios), reflecting principally the surface area of the nanometer-sized intra-columnar pores in this case.

This study presents the analysis of pore surface area changes during the ageing of EB-PVD top coat materials by SANS, Brunauer–Emmett–Teller (BET) and scanning electron microscopy (SEM). The results are discussed comparing the nature of these changes with those of nano-particles and pores. Due to the nanometer size, difficulty of accessibility, complex morphology as well as internal energy of the different elements present in the columnar structure of the EB-PVD coatings (i.e. solid state phase and porosity), a combination of innovative analysis techniques is required to determine the atomic diffusion mechanisms activated by exposing the material to high temperatures. In order to define the governing diffusion mechanism and its activation energy, changes in the surface area ($\Delta S/S_o$) of the different porosity types after isothermal ageing at 1100 °C for various times as well as at different temperatures varying from 900 °C to 1400 °C for a constant holding time were measured. The analysis of the measured properties which are provided using a constant heating-rate during heat treatment minimizes experimental problems with shifting in atomic transport mechanisms.[5]

2. Methods and materials

2.1. Processing

After the corresponding cleaning of the flat metallic Ni-basis super-alloy substrates (IN718), NiCoCrAlY bond coats were vapour phase deposited followed by peening and vacuum annealing. Additionally, top coats based on partially yttria stabilized zirconia (PYSZ) were deposited via EB-PVD process using a 150 kW pilot plant (von Ardenne, Germany), a detailed description of which is given elsewhere.[18,19] The substrates were mounted on a rotating horizontal holder positioned perpendicular to the ingot axis and coated under conventional rotating mode.[20] Oxygen flow into the coating chamber was adjusted to obtain the desired vacuum and uphold the stoichiometry at the coatings. The evaporation source material was a 63.5 mm diameter ingot provided by

Transtec (TT, USA) with standard ZrO_2–7 to 8 wt.% Y_2O_3 chemical composition.

Deposition of the PYSZ top coating was carried out by single source evaporation by applying an electron power gun of 70 kW and 8×10^{-3} mbar chamber pressure. During the process the substrates were rotated at a speed of 12 min^{-1} and heated to 950 °C. Using these parameters, a deposition rate of 6.3 μm/min was achieved resulting in a coating thickness of 400 μm. After deposition, the coatings were separated from substrate and bond coat by chemical etching. The free-standing coating specimens were subsequently aged in air at 1100 °C for 20 min, 1 h, 3 h, 10 h and 100 h and at temperatures 900 °C, 1000 °C, 1100 °C, 1200 °C, 1300 °C and 1400 °C for 1 h. For each given ageing condition, one single specimen was employed for further characterization.

2.2. Characterization

BET method was employed to measure the surface area from the open porosity and SANS method for the open and closed pores smaller than 180 nm by determining the apparent Porod surface area. The BET measurements were carried out at the Department of Ceramic Technologies and Sintered Materials of the Fraunhofer Institute in Dresden by using an accelerated surface area porosimeter system (ASAP 2010) and employing N_2 as analysis gas. The corresponding dimensions of the utilized specimens were 7 mm (width) × 20 mm (length) × 400 μm (thickness).

The SANS measurements were performed at the time-of-flight small angle neutron diffractometer (SAND) at the Intense Pulsed Neutron Source (IPNS) of Argonne National Laboratory. Detailed description is given elsewhere.[21] The sample-to-detector distance was 2 m and the q range 0.035–6 nm^{-1}. Each measurement was carried out on one specimen having the dimensions of 0.4 mm × 7 mm × 15 mm after ageing at above given temperatures and times. These specimens were placed on a sample holder using a cadmium mask with a circular slit of 5 mm diameter. Under the measurement conditions, the analysed volume of the specimens was 5 mm × 0.4 mm (diameter × thickness). The data were corrected for background and empty cell scattering.

For the BET and SANS methods, the specimens were analysed in free-standing condition in order to avoid measurements of entities different from the TBC top coat, since the incident beam interacts with the specimen along the plane perpendicular to the substrate (i.e. parallel to the column axis) as the scattered neutron intensity was determined.

The microstructures were characterized using a field-emission scanning electron microscope (FE-SEM, LEITZ LEO 982).

3. Results and discussion

The reduction in the surface energy is the driving force for sintering and induces changes in the surface area of pores. This modifies the morphology until the lowest surface area is reached for a corresponding volume resulting in an equilibrium shape.[22,23] For the as coated EB-PVD top coat, it is evident that the shape of the open and closed pores is far from the equilibrium as is shown by the left and right inserted micrographs in Fig. 1.

The surface temperatures of the turbine blades at current aircraft engines range between 1100 °C and 1200 °C, therefore, isothermal ageing of specimens were carried out at 1100 °C for exposure times varying between 20 min and 100 h. The analysis of these results can help to provide information about the influence of time and thus, on the sintering kinetics of TBC top coats analogue to those obtained for the powder compacts.[4] As Fig. 2 demonstrates, significant surface area changes were observed in the total open and closed porosity of the coatings within the first minutes of ageing at 1100 °C exceeding the 50% limit given in German's model.

Scanning electron microscopy investigations of the coatings aged for 1 h at 1100 °C showed that feather-arm features and intra-columnar closed porosity became coarser in comparison with those in the as-coated state (Fig. 3, top left and bottom). In contrast, no considerable porosity changes were observed in the coatings on further ageing for 100 h at 1100 °C (Fig. 3, top right). It appears that the atomic diffusion started already during the heating period before the exposure temperature was reached. It is evident that the surface area

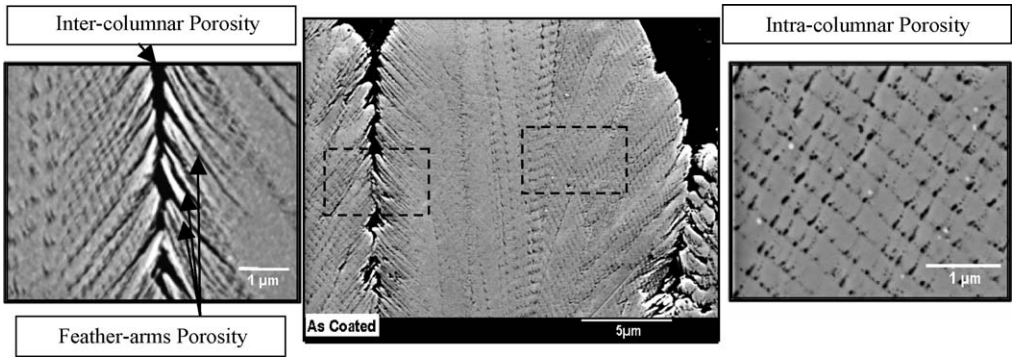

Fig. 1. Scanning electron micrographs of the cross sections of EB-PVD PYSZ top coats displaying the columnar microstructure in as-coated state (middle), containing inter-columnar and feather-arm porosity (left) and intra-columnar pores (right).

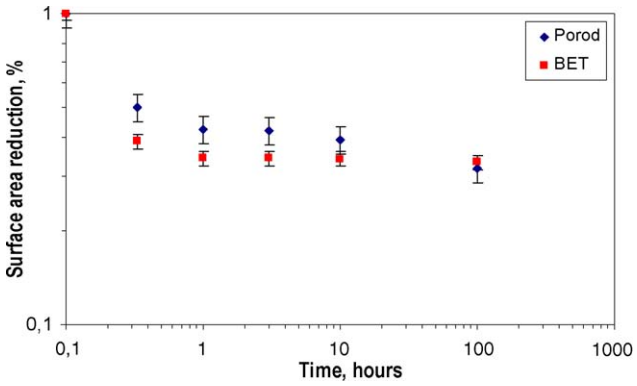

Fig. 2. Surface area reduction of open (measured by BET) and closed pores (calculated by SANS) after ageing of EB-PVD top coats at 1100 °C for various times. Deviations from the calculated values of the surface area using the data fitting process are represented by the vertical bars. These were ±10% for Porod (SANS) and ±5% for BET-measurements.

configuration of the open and closed pores after ageing for 1 h at the given temperature reaches a partial equilibrium (i.e. smoothness) state. Such partial equilibrium is more pronounced in open pores (as measured by BET) than in closed ones (determined by SANS) (see Figs. 2 and 3). It indicates that the chemical potential present at the curvature of the pore surfaces is not high enough to drive atomic diffusion within a reasonable time at the mentioned temperature. Analogous results were found by Akash et al.,[24] who demonstrated that an equilibrium (smoothing) value for the pores at tetragonal structured 3 mol.% YSZ powder compacts was reached after different but defined lengths of time at various ageing temperatures, if sintering is governed solely by surface diffusion. Moreover, Gregory et al.[25] stated that in the case of pores with a non-equilibrium morphology, transfer of atoms must occur from rough to smooth surfaces. For occurrence of material transfer between different surface morphologies, a nucleation energy barrier must be overcome. If this barrier is not overcome, the morphology change of the pores will be achieved only at a fraction of the final equilibrium shape.

In our experimental case, it was not possible to apply this proposed model to determine the governing sintering mechanism due to the rapid sintering kinetics of EB-PVD top coats at the above given temperature. Therefore, other influencing factors were considered.

The changes in activation energy also deliver information about the occurrence of different sintering mechanisms and can be determined by isothermal ageing of coatings at different temperatures for a constant exposure time and by heating at a constant rate.[5,6] Fig. 4 shows the changes in surface area reduction ($\Delta S/S_o$) as a function of temperature using a constant heating rate of 5 °C/min. The graph in Fig. 4

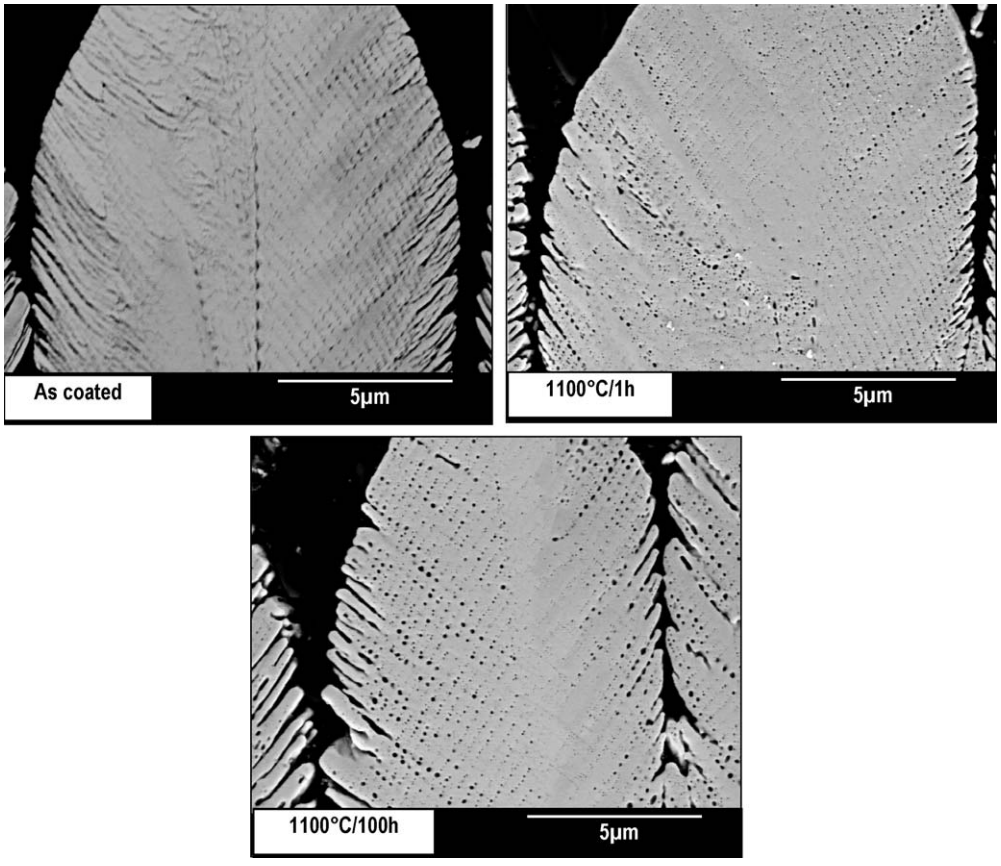

Fig. 3. Scanning electron micrographs of the cross sections of the EB-PVD standard top coat displaying the morphological changes in the columnar microstructure in as coated state (left) and after ageing at 1100 °C for 1 h (right) and for 100 h (bottom).

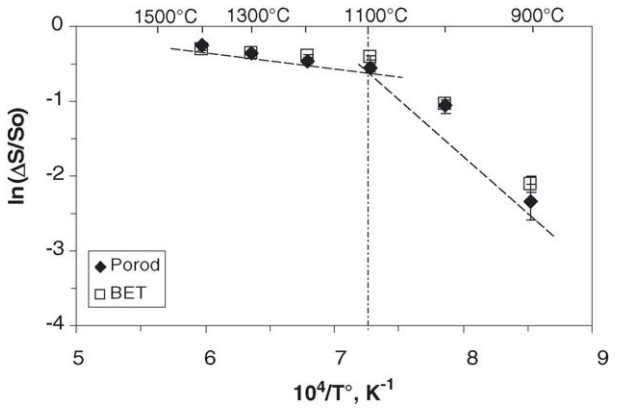

Fig. 4. Surface area reduction data plotted against temperature is used as a basis to calculate the apparent activation energy for surface area loss with a heating rate of 5 °C/min. Deviations from the calculated values of the surface area using the data fitting process are represented by the vertical bars. These were ±10% for Porod (SANS) and ±5% for BET-measurements.

implies that the sintering process begins at 900 °C, considering the surface area of the coatings after one hour ageing at 900 °C (4.8 $m^2/g \pm 10\%$) and the initial surface area of the coatings as-coated state (5.2 $m^2/g \pm 10\%$). Similar results were reported by Fritscher et al.[26] The curve given in Fig. 4 also displays a change in the slope at about 1100 °C. The surface area changes of the different pore types present in the EB-PVD top coats occur rapidly in the temperature range of 900 °C–1100 °C. For a precise analysis, employment of in situ SANS measurements may be necessary. Above 1100 °C, the rate of surface area reduction diminishes drastically indicating a change in the driving force and/or the diffusion mechanism for the sintering process.

Microstructural observation of the coatings aged at different temperatures for one hour shows that substantial changes in the morphology and distribution of the porosity occur at temperatures between 900 °C and 1100 °C. Considering the slope change in Fig. 4, one can assume that the morphological alteration becomes rather insignificant in the temperature range between 1100 °C and 1400 °C. In spite of the rate reduction in the surface area change in the second half of the curve of Fig. 4, considerable microstructure change is noticeable at the coatings aged for one hour at temperatures between 1100 °C and 1400 °C as shown in Fig. 5.

Using the equation suggested by German,[5] the ratios between the activation energy and the mechanism constant (Q/γ) for the two different slopes of the curve were calcu-

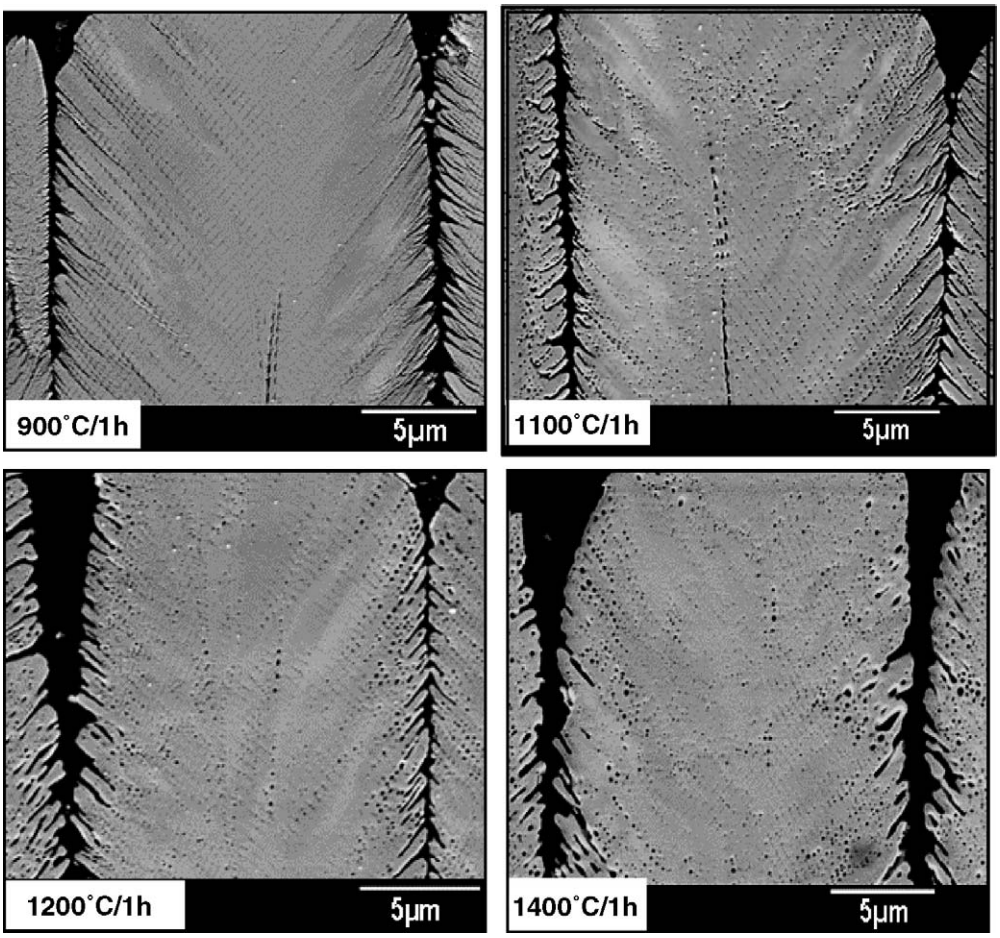

Fig. 5. Scanning electron micrographs of the cross sections of the EB-PVD standard top coats showing the changes in columnar after annealing for one hour at 900 °C (top left), 1100 °C (top right), 1200 °C (down left) and 1400 °C (down right).

lated. At the temperature range of 900 °C–1100 °C, these yield average calculated (Q/γ) ratios of 114 kJ/mol and 120 kJ/mol for the BET and SANS data, respectively. According to the investigations carried out on solid state sintering of 3 mol.% Y_2O_3–ZrO_2 powders in air revealed that three different atomic diffusion mechanisms were operating. These are referred to as surface, lattice/volume and grain-boundary diffusions.[24,27,28] The grain boundary diffusion can be ruled out for the EB-PVD top coats since their morphological build-up at the as-coated state displays no grain boundary development. The columns of EB-PVD PYSZ coating are *quasi* single crystals having tetragonal crystal structure. Comparing the calculated (Q/γ) ratios with those of the literature data,[5,6] one can postulate that the surface diffusion (120 kJ/mol) is the most suitable diffusion mechanism to occur during ageing of EB-PVD PYSZ coatings at the temperature range of 900 °C and 1100 °C. Similar results were previously reported by Lughi et al.[2]

At the temperature range of 1100 °C–1400 °C, the surface area reduction exceeds the limit of applicability of the model used, and thus, may result in no rational fitting of the data to one single possible sintering mechanism. It is likely that at this second stage more than one diffusion mechanisms occur simultaneously.

The presence of complex pore morphologies in EB-PVD manufactured PYSZ top coats should be regarded for interpretation of the influence of surface diffusion on pore morphology changes and consequently on sintering. It is likely that in different pore groups different morphological changes occur although the driving force for their initiation might be the same, namely surface diffusion.

Considering the conclusions drawn by Bullard and Searcy[29] that the surface diffusion is the principal path of mass transport between the facets of a cross section which lies in the range of 5 μm–100 μm, the significance of the occurrence of this mechanism at the inter-columnar pores of EB-PVD thermal barrier top coats becomes perceptible.

Transition state theory applies for both diffusion-limited shape changes and attachment–detachment–limited shape changes. Bullard and Searcy[30] state that whenever both convex and concave facets are present on a crystalline surface, these edges provide favourable sites for formation of monolayer ledges at which detachment and attachment of molecules (or atoms) can occur. Dramatic differences take place by complex shapes with time when surface diffusion is rate-limiting or detachment of atoms from a source facet at a sink facet is rate-limiting.[31] Thus, it is reasonable to assume that the coarsening of the feather-arm feathers is a result of surface diffusion driven matter transport leading to detachment/attachment process from convex to concave facets which is rate-limiting.

For the isolated voids which may remain from the initially continuous porosity network, surface diffusion, if rapid, can provide sufficient mobility that those pores may migrate.[29] Stability/instability of small objects correlates with the size dependence of the specific surface excess free energy $\sigma(R)$.[32] In the case of isotropic specific surface energy, a particle or void shape will change to spheres of the same volume. In an assembly of identical pores with the smallest surface to volume ratio and isotropic surface energy, no change in the microstructure will occur during sintering, due to the absence of differences in bonding environment.[33] On the other hand, on edges and corners the atoms exhibit a different bonding environment when compared to atoms located on faces. Their bonding environment will change in order to decrease the energy and to ensure the most possible uniformity.[33] Pores and particles with anisotropic surface energies will often persist in metastable shapes.[34] Achievement of equilibrium starting with these nano-sized shapes may, nevertheless, require either longer exposure time than that applied in this study or higher temperatures than those of present service temperatures.

4. Conclusions

The model developed by German et al.[5] to determine the governing sintering mechanism in powder compacts seems to be well suited for the EB-PVD PYSZ top coats within its $\Delta S/S_o \approx 50\%$ surface area reduction applicability limit. According to this, the obtained results indicate that atomic diffusion mechanism in the temperature range of 900 °C–1100 °C is surface diffusion. However, at the temperature range 1100 °C and 1400 °C, it was not possible to determine one single mechanism. It is likely that at this range more than one diffusion mechanisms take place. Surface diffusion occurring at the temperature range of 900 °C–1100 °C may be the cause for migration of small pores as well as matter transport from convex to concave sites.

Sintering starts already at 900 °C for the studied coating, manufactured by applying standard process parameters and aged under given conditions. At 1100 °C, pore surface morphology seems to reach a partial equilibrium shape after one hour. According to the Wulff theory,[35] achievement of fully equilibrium shape can not be possible within a reasonable time, although, due to the differences in their bonding environment, the pores with anisotropic surface energies or those with curved surfaces having chemical potential differences may become metastable.

Acknowledgments

The authors acknowledge the conscientious assistance of C. Kröder, J. Brien, and H. Mangers of DLR in the production of the coatings. We also would like to express our gratitude to Dr. C.-K. Loong, Dr. G. Liang, and D.G. Wozniak for their support with the SANS measurements at the Intense Pulsed Neutron Source (IPNS) of Argonne National Laboratories (ANL), USA.

References

1. Azzopardi, A. *et al.*, Influence of aging on structure and thermal conductivity of Y-PSZ and Y-FSZ EB-PVD coatings. *Surf. Coat. Technol.*, 2004, **177–178**, 131–139.
2. Lughi, V., Tolpygo, V. K. and Clarke, D. R., Microstructural aspects of the sintering of thermal barrier coatings. *Mater. Sci. Eng. A*, 2004, **368**(1–2), 212–221.
3. Kingery, W. D., Bowen, H. K. and Uhlmann, D. R., *Introduction to Ceramics* (*2nd ed.*). John Wiley and Sons, New York, 1976, p. 1017.
4. German, R. M. and Munir, Z. A., Surface area reduction during isothermal sintering. *J. Am. Ceram. Soc.*, 1976, **59**(9–10), 379–383.
5. German, R. M., *Sintering Theory and Practice*, ed. John, I. Wiley and Sons, Wiley-Interscience, New York, NY, 1996.
6. Hillman, S. H. and German, R. M., Constant heating rate analysis of simultaneous sintering mechanisms in alumina. *J. Mater. Sci.*, 1992, **27**, 2641–2648.
7. Sen, D. *et al.*, Pore morphology in sintered ZrO_2–8% mol Y_2O_3 ceramic: a small-angle neutron scattering investigation. *J. Alloys Compd.*, 2002, **340**, 236–241.
8. Sen, D. *et al.*, Pore growth during initial and intermediate stages of sintering in ZrO_2–3 mol.% Y_2O_3 compact: a small-angle neutron scattering investigation. *J. Alloys Compd.*, 2003, **361**(1–2), 270–275.
9. Sen, D. *et al.*, Effect of sintering temperature on pore growth in ZrO_2–8 mol.% Y_2O_3 ceramic compact prepared by citric acid gel route: a small-angle neutron scattering investigation. *J. Alloys Compd.*, 2004, **364**(1–2), 304–310.
10. Harmat, P. *et al.*, Sintered materials studied by small-angle neutron scattering. *Physica B*, 2000, **276–278**, 826–829.
11. Krueger, S., Long, G. G. and Page, R. A., Characterization of the densification of alumina by multiple small-angle neutron scattering. *Acta Crystallogr.*, 1991, **A47**, 282–290.
12. Allen, A. J. *et al.*, Microstructure evolution during sintering of nanostructured ceramic oxides. *J. Am. Ceram. Soc.*, 1996, **79**(5), 1201–1212.
13. Allen, A. J. *et al.*, Small-angle neutron scattering studies of ceramic nanophase materials. *Nanostruct. Mater.*, 1996, **7**(1–2), 113–126.
14. Allen, A. J. *et al.*, Microstructural characterization of yttria-stabilized zirconia plasma-sprayed deposits using multiple small-angle neutron scattering. *Acta Mater.*, 2001, **49**(9), 1661–1675.
15. Porod, G., In *Small-angle X-ray scattering*, ed. O. Kratky. Academic Press, London, U.K, 1982. pp. 17–51.
16. Ilavsky, J., Allen, A. J. and Long, G. G., Characterization of the closed porosity in plasma-sprayed alumina. *J. Mater. Sci.*, 1997, **32**, 3407–3410.
17. Hall, P. J. *et al.*, The effects of the electronic structure of micropores on the small angle neutron scatering of X-rays and neutrons. *Carbon*, 2000, **38**, 1257–1259.
18. Kaysser, W. A., et al. *Processing, characterisation and testing of EB-PVD thermal barrier coatings*. AGARD-R-823, 1998.
19. Lenk, P., Senf, J. and Wenzel, B.-D., Thermal barrier coating-A new application for von Ardenne guns. *EB-PVD Workshop*. University Park State College, Pennsylvania, 1996.
20. Schulz, U., Terry, S. G. and Levi, C. G., Microstructure and texture of EB-PVD TBCs grown under different rotation modes. *Mater. Sci. Eng. A*, 2003, **360**(1–2), 319–329.
21. Thiyagarajan, P. *et al.*, The time-of-flight small-angle neutron diffractometer (SAND) at IPNS, Argonne National Laboratory. *J. Appl. Cryst.*, 1997, **30**, 280–293.
22. Kirkaldy, J. S. and Young, D. J., *Diffusion in the Condensed State*. The Institute of Metals, London, 1987.
23. Adam, N. K., *The Physics and Chemistry of Surfaces* (*3rd ed.*). Oxford University Press, London, 1949.
24. Akash, A. and Mayo, M. J., Zr surface diffusion in tetragonal yttria stabilized zirconia. *J. Mater. Sci.*, 2000, **35**, 437–442.
25. Roher, G. S., Roher, C. L. and Mullins, W. W., Nucleation energy for volume-conserving shape changes of crystals with nonequilibrium morphologies. *J. Am. Ceram. Soc.*, 2001, **84**(9), 2099–2104.
26. Fritscher, K., et al. Aspects on sintering of EB-PVD TBCs. In *Seventh International Symposium on Ceramic Materials and Components for Engines*. Wiley-VCH, Goslar, 2000.
27. Akash, A. and Mayo, M. J., Pore growth during initial-stage sintering. *J. Am. Ceram. Soc.*, 1999, **82**(11), 2948–2952.
28. Duran, P. *et al.*, Low-temperature sintering and microstructural development of nanocrystalline Y-TZP powders. *J. Eur. Ceram. Soc.*, 1996, **16**(9), 945–952.
29. Bullard, J. W. and Searcy, A. W., Microstructural development during sintering of lithium fluoride. *J. Am. Ceram. Soc.*, 1997, **80**(9), 2395–2400.
30. Bullard, J. W. and Searcy, A. W., Equilibria and kinetics of mass transport between crystal facets: a comparison of two models. *Acta Mater.*, 1999, **47**(10), 3057–3061.
31. Carter, W. C. *et al.*, Shape evolution by surface diffusion and surface attachment limited kinetics on completely faceted surfaces. *Acta Metall. Mater.*, 1995, **43**(12), 4309–4323.
32. Samsonov, V. M., Sdobnyakov, N. Y. and Bazulev, A. N., On the thermodynamics stability conditions for nanosized particles. *Surf. Sci.*, 2003.
33. Drofenik, M., Grain size and conductivities anomaly in donor-doped barium titanate. *Acta Chim. Slov.*, 1999, **46**(3), 355–364.
34. Searcy, A. W., Driving force for sintering of particles with anisotropic surface energies. *J. Am. Ceram. Soc.*, 1985, **68**(10), C-268–C-276.
35. Wulff, G., Zur Frage der Geschwindigkeit des Wachstums und der Auflösung der Krystallflaechen. *Z. Kristallogr.*, 1901, **34**, 449–530.